Materials Research Innovations

ISSN: 1432-8917 (Print) 1433-075X (Online) Journal homepage: http://www.tandfonline.com/loi/ymri20

Experimental research on aluminium–magnesium fuel-rich propellant under high strain rates

J. Zheng, W. Wang, X. Chen, C. Zhou & J. Xu

To cite this article: J. Zheng, W. Wang, X. Chen, C. Zhou & J. Xu (2015) Experimental research on aluminium–magnesium fuel-rich propellant under high strain rates, Materials Research Innovations, 19:sup8, S8-245-S8-250

To link to this article: http://dx.doi.org/10.1179/1432891715Z.0000000001668

Published online: 18 Nov 2015.

Experimental research on aluminium–magnesium fuel-rich propellant under high strain rates

J. Zheng*, W. Wang, X. Chen, C. Zhou and J. Xu

The aluminium–magnesium fuel-rich propellant is one of the classified propellant used in the solid rocket ramjet. The weapons with the rocket ramjet are under high overload by launching, the mechanical properties of the propellant should be studied under high strain rate. The uniaxial compressive mechanical curves of the aluminium–magnesium fuel-rich propellant under high strain rates have been obtained with the modified split Hopkinson pressure bar in this paper. Four groups of stress–strain curves were obtained at different strain rates of 2600, 3300, 4500 and 5100 s^{-1}. The experimental results show that the mechanical properties of the aluminium–magnesium fuel-rich propellant are rate-dependent, and the Mg–Al fuel-rich propellant has the mechanical properties of viscoelastic material. With the increase of strain rate, the modulus of the aluminium–magnesium fuel-rich propellant obviously increases. The underlying mechanism of the significant rate sensitivity was investigated by adopting the scanning electron microscope from a micro-structure point of view.

Keywords: Experimental research, Fuel-rich propellant, High strain rate, Mechanical properties, Solid rocket ramjet, Viscoelastic material

Introduction

Fuel-rich propellant is mainly used in solid ducted rocket, solid fuel ramjet, new solid–liquid hybrid rocket and air turbo rocket to improve combustion efficiency. Relative to the solid rocket propellant, fuel-rich propellant antioxidant levels is much lower. In general, its antioxidant content should be kept above the floor level to make it can realise a normal decomposition combustion before the secondary combustion. The composition of fuel-rich propellant is similar to the common components of a composite propellant, mainly including adhesive fuel, metal/nonmetal fuel and oxidant. By using the main fuel composition, the fuel-rich propellant can mainly be classified into three kinds: hydrocarbon fuel-rich propellant, metal fuel (including magnesium, aluminium and their combination) fuel-rich propellant and boron fuel-rich propellant.[1]

After decades of development, the performance of the fuel-rich propellant is continuously improved, and its formulation types appear diversified development. Many scholars, at home or abroad, have done a lot of research in the formulation and performance adjustment of the fuel-rich propellant. Liu *et al.*[2] studied the effect of different content of cyclonite (RDX), cyclotetramethylenetetranitramine (HMX), potassium nitrate and potassium perchlorate (KP) on the burning rate and combustion temperature of the boron-based fuel-rich propellant. High-pressure differential scanning calorimetry (DSC) and simultaneous thermogravimetry (TG)/DSC were used to study the different kinds of boron that was used in the fuel-rich propellant. Also, some of the samples before the experiment and after the experiment were analysed by the scanning electron microscope (SEM).[3,4] Wang *et al.*[5–9] researched the temperature distribution of combustion wave and the quench combustion experiments for two boron-based fuel-rich propellants under low pressure, and analysed the quenched surfaces of the propellants with SEM and energy dispersive spectrometer. Kakami measured the burning rates of hydroxyl-terminated polybutadiene (HTPB) and ammonium-perchlorate composite solid propellants at pressures up to 90 kPa under laser irradiation, and propellant-pre-heat temperature distribution by thermography. Combustion control, including ignition and interruption by laser irradiation, was feasible for solid fuel-rich propellants with a burning rate coincident with Vieille's law and a pressure exponent of approximately 0·5.[10] Brewster studied the flame structure in wide-distribution ammonium-perchlorate (AP), aluminium (Al), HTPB binder and composite propellants using 2-D laminates with oxygenated binder. The flame structure is found to be similar to that previously described using ultraviolet and infrared imaging for non-aluminised laminates with split flame structure at high pressures and low fuel thicknesses and merged flame structure for low pressure and low fuel thicknesses.[11]

School of Mechanical Engineering, Nanjing University of Science & Technology, 200 Xiaolingwei Street, Nanjing 210094, China

*Corresponding author, email zhengjian@njust.edu.cn

Received 13 September 2014; accepted 20 October 2014
DOI 10.1179/1432891715Z.0000000001668

And at present the aluminium–magnesium fuel-rich propellant has wide applications because of its high energy density and technology maturity. This kind of solid propellant is consisted of AP, KP, Al, magnesium powder (Mg) and HTPB binder.[1] It is filled with a large number of solid granules. So its performance has been discussed and investigated by a number of scholars.

Zhang systematically investigated the combustion properties of the Mg/Al fuel-rich propellant. The results showed that increasing the oxidiser content and the Mg/Al ratio can remarkably enhance the burning rate and pressure exponent, but it is unfavourable to the performance of the propellant. Careful selection and combination of the oxidiser and metal particle size is the best way to modify the combustion properties of the fuel-rich propellant. Addition of KP can increase the burning-rate exponent effectively.[12] Xiao studied the quenched surfaces of three kinds of solid fuel-rich propellants with same content of magnesium–aluminium alloys (with mass ratio of 1:1), magnesium/aluminium powder (with mass ratio of 1:1) and aluminium powder by SEM. At the same time, the images of combustion structures were used to research the differences of three kinds of metal fuels. Experiments validated that the combustion efficiency of magnesium–aluminium alloys is higher than the other two propellants.[13] Pang and Fan[14] determined the combustion heat of Mg/Al fuel-rich propellant by means of constant temperature with apparatus of oxygenic bomb calorimeter, and analysed the effected factors about the testing uncertainties of propellant. Huang adopted a high-pressure combustor and a metal/steam reactor to simulate the two-stage combustion of a Mg-based fuel-rich propellant used for water ramjet engines. The solid combustion products from the two stages were collected and characterised by SEM. In addition, the thermal properties of the solid products of the primary combustion were characterised by differential thermal analysis and simultaneous TG. The burning rates at different pressures were measured by high-speed cinematography.[15] Singh studied the burning rate and energetics of Mg–$NaNO_3$ and Zr–$NaNO_3$ metal-based propellants to elucidate their combustion mechanism and to understand the influence of addition of Zr particles on the combustion of Mg–$NaNO_3$ system at different oxidiser levels. Results indicated that the burning rate of Mg–$NaNO_3$ and Zr–$NaNO_3$ propellants is higher at fuel-rich ratio because of high-condensed phase heat release and decreases with increasing oxidiser content. It shows a minimum value at stoichiometric ratio because of formation of metal agglomerates at the burning surface.[16]

Pang *et al.*[17] investigated the micro-structures and granularity distribution of different metal particles and the energy, sensitivity and combustion properties of fuel-rich solid propellants with different metal particles in detail. It was found that the magnesium particles are more uniform than other metal powders. Liao determined the physic-chemical characteristics of spherical and coarse magnesium particles and evaluated the burning-rate performance and mechanical properties of the fuel-rich propellant.[18,19]

The research done by the scholars in front is concentrated in the propellant formula, component content, combustion characteristic of the magnesium–aluminium fuel-rich propellant, rarely involves the mechanical properties of it, especially the mechanical properties under high strain rate.

As the technical requirements of modern rocket weapons for the solid rocket motor become higher and higher, the solid propellant loading is asked to support not only the static loading, such as its own weight and the extrusion by motor's hull, but also the dynamic loading, such as vibrating, temperature cycle, transient pressure impact by ignition and dynamic high overload. These span not only the static state under constant temperature but also high strain rates. Because the mechanical properties of propellant are sensitive to the strain rate, it is necessary and quite important to study the mechanical responses at different strain rates.[20] Such studies can help us analyse the complex stress conditions of the rocket ramjet and provide a theoretical basis for the design of the solid rocket ramjet.

In this paper, the tests of the Mg–Al fuel-rich propellant specimens are performed under high strain rate by using the split Hopkinson pressure bar (SHPB) system for the first time. The uniaxial compressive mechanical curves of this propellant are obtained under five different strain rates. From the experimental results, we can learn the influence of strain rate on the mechanical characteristics of this propellant. Also, some of the specimens before the test and after the test are analysed by SEM. In combination with the SEM images of the specimens, from the micro-perspective, the deflection of the propellant specimens structure is illustrated under the action of high overload, and its mechanical characteristics are illuminated by changing with the strain rate.

Experimental procedure

Material and specimens

The material of the Mg–Al fuel-rich propellant tested in this paper is constituted by AP as oxidants, Mg–Al powders as fuel additives, HTPB as binders, and other additives such as plasticisers, cross-linkers, curing agent and stabiliser. Its formula and content are shown in Table 1.

The Mg–Al fuel-rich propellant is a kind of soft solid composite, so establishing the proper shape and size of the specimen is crucial for the effectiveness of the test data. Some correlative studies have been done by many scholars on the SHPB test for soft material. Kolsky and Forrestal conducted some tests about soft specimens at high strain rates. They pointed out that the assumption of uniform stress in the specimen was not appropriate for thick specimens in dynamic experiments.[21,22] Dioh *et al.*[23] did a study on the influence of polymer specimens' thickness in the high strain rate tests. Gray and Blumenthal[24] supported the work in traditional SHPB tests, by showing that soft material could achieve the balance of stress only in later stages. Chen recorded the deformation process of thick rubber specimens in SHPB tests with a high-speed camera. Reducing the

Table 1 Formulations of the Mg–Al fuel-rich propellant

Substance constitution, % (weight)			
AP	Mg–Al powders	HTPB	Other additives
30	40	25	5

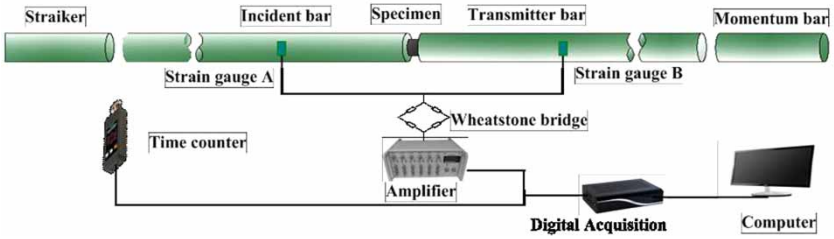

1 Schematics of the split Hopkinson pressure bar (SHPB) system

thickness of specimens is conducive to achieving stress equilibrium, but if the ratio of length to diameter is too small, the friction effect will increase and influence the test result.[25] The specimen adopts the shape of the disc with its diameter of 10 mm and the length of 4 mm in this paper.

Experimental set-up

The SHPB set-up is an ideal machine to study dynamic mechanical properties of materials. However, the set-up should be modified according to material properties as well as the different test conditions. The uniaxial compression experiments under high strain rates are tested using the modified SHPB system (Fig. 1). The SHPB set-up is composed of a striker (300 mm in length), an incident bar (1400 mm in length), a transmitted bar (1400 mm in length) and a momentum bar (400 mm in length), made of high-strength aluminium alloy LC4 with a density of 2740 kg m^{-3} and a nominal modulus of 74 GPa. Strain gauges are mounted at 700 mm away from the bar/specimen interfaces on the incident bar and transmitted bar connecting to a 12-bit digital oscilloscope through a Wheatstone bridge and a differential amplifier (CS-1D dynamic strain meter) to monitor incident pulse $\varepsilon_i(t)$ and transmitted pulse $\varepsilon_t(t)$, respectively. The distances of strain gauges on the incident bar and the transmission bar to the specimen are 700 mm.

To increase the width of the loading wave, the length of the striker bar is chosen to be 400 mm. The effect of the pulse shaper is to decrease the oscillation of the wave in the bar. Based on the speed of the striker bar, the thick card is select as the pulse shaper.

Data processing

As the experiment performed, the striker that is launched by the gas gun generated an incident pulse of an approximate duration of 250 μs. The striking velocity was measured by a time counter and a data acquisition unit measurement system. All of the raw data just as observed on digital oscilloscope were processed after being digitally filtered using a low-pass filter with a cut-off frequency of 10 MHz. The recorded pulses were converted into strains to determine the normal force history of the specimen, and calculated by computer finally.

Two-wave method is widely used in the test results processing of various materials. It is based on one-dimensional assumption and the assumption of uniformity. In accordance with the one-dimensional stress wave theory, the average strain rate $\dot{\varepsilon}(t)$, the average strain $\varepsilon(t)$ and the average stress $\sigma(t)$ of both ends of the specimen during testing can be expressed as

$$\begin{cases} \dot{\varepsilon}(t) = \dfrac{C_0}{l_s}(\varepsilon_I - \varepsilon_R - \varepsilon_T) \\ \varepsilon(t) = \dfrac{C_0}{l_s}\int_0^t (\varepsilon_I - \varepsilon_R - \varepsilon_T)\mathrm{d}t \\ \sigma(t) = \dfrac{E_0 A_0}{2A_s}(\varepsilon_I + \varepsilon_R + \varepsilon_T) \end{cases} \quad (1)$$

where $\varepsilon_I(t)$, $\varepsilon_R(t)$, $\varepsilon_T(t)$ are respectively the strain history of the incidence wave, the reflected wave and the transmitted wave of pressure bar. C_0, E_0, A_0 are respectively the wave velocity, elastic modulus and cross-sectional area of the elastic bar. l_s and A_s are respectively the length and the origin cross-sectional area of the specimen.

If the uniformity assumption of the specimen is introduced, the above equations can be simplified as

$$\begin{cases} \dot{\varepsilon}(t) = \dfrac{2C_0}{l_s}\varepsilon_R(t) \\ \varepsilon(t) = \dfrac{2C_0}{l_s}\int_0^t \varepsilon_R(t)\mathrm{d}t \\ \sigma(t) = \dfrac{E_0 A_0}{A_s}\varepsilon_T(t) \end{cases} \quad (2)$$

Equation (2) is the classic two-wave method test data processing formulas. In this paper, all the stress–strain curves are processed by two-wave method using the transmitted wave and the reflected wave.[26,27]

Experimental results

Analysis of the dynamic compressive experiment

According to the theory of the stress wave, the SHPB test needs to satisfy the assumption of one-dimensional stress and uniform stress. In addition, in order to study the effect of strain rate on mechanical properties of the material, it is necessary to understand the constant strain rate loading. So it is necessary to test and verify the effectiveness of the dynamic data before studying mechanical properties of materials. Figure 2 shows a set of waveforms obtained at room temperature. The incident wave signal and reflected wave signal are magnified 200 times. Owing to the fuel-rich propellant material is soft, the transmitted signal is not obvious, the transmission wave signal is magnified 500 times. The incident wave is similar to a bilinear-wave, which is beneficial to the achievement of stress uniform and constant strain rate. The reflected wave is a trapezoidal wave, which can generate an ideal platform to determine the deformation process at a constant strain rate of the specimen.

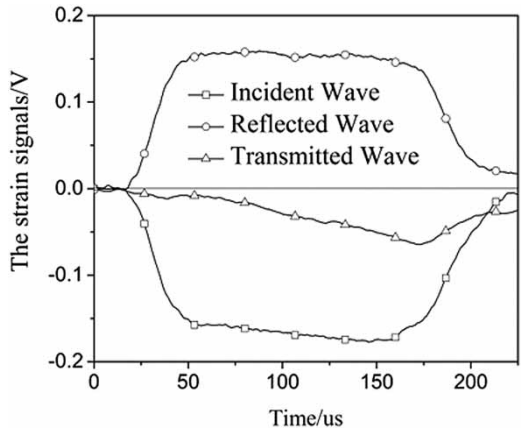

2 The stress wave signals obtained in test

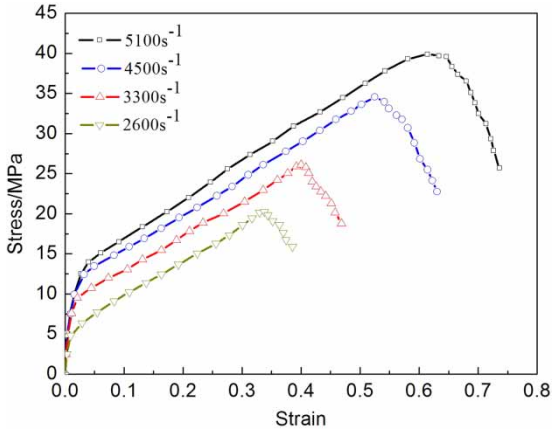

3 The stress–strain experimental curves of 293 K at different high strain rates

The stress wave signals shown in Fig. 3 allow us to obtain the axial stress histories of the specimen's two ends by the two-wave method. The high strain rate tests are performed on the modified SHPB set-up. According to the test conditions and material properties, four groups of mechanical curves can be obtained at different high strain rates (2600, 3300, 4500 and 5100 s^{-1}). At least five groups of tests are performed under the same conditions, and then we get an average result for each condition. Figure 3 shows the mechanical curves of the Mg–Al fuel-rich propellant of 293 K at different high strain rates. The Mg–Al fuel-rich propellant is obviously rate-dependent at the high rates, and with the increasing strain rate, the modulus increases. The stress of the Mg–Al fuel-rich propellant increases with the increase of the strain, having no obvious yield phenomenon, and it is similar to the mechanical properties of solid rubber filling materials. The Mg–Al fuel-rich propellant at high strain rates can also produce a larger viscoelastic deformation, and it indicates this fuel-rich propellant has the mechanical properties of viscoelastic material.

Results from SEM analysis

Figure 4 shows the macro-picture of the specimens after the different strain rate tests. From the contrast analysis of the specimens tested at four strain rates, we found that with the increase of strain rate, the greater extend of the specimens were compressed. At the strain rate of 2600 s^{-1}, the cylindrical specimen was compressed to a certain extent, but does not appear the cracks around its surface. With the increase of strain rate, the surface of the specimen appears the cracks. The specimen were crushed at the strain rate of 5100 s^{-1}.

In order to explain the rate dependence of the Mg–Al fuel-rich propellant better, we adopt the SEM to investigate the underlying mechanism of the significant rate sensitivity from a micro-structure point of view. Figure 5 presents the typical SEM micrographs of compression surface for the specimens at high strain rates (2600, 3300 and 4500 s^{-1}). As the specimen has been crushed at the strain rate of 5100 s^{-1}, its SEM micrograph cannot provide. Figure 5 gives a high magnification (×100) of a part of overall surface morphology. Evidence from SEM indicates that the AP particles do not fracture, and some cavities and voids are also observed. These AP particles structure is characteristic of the interaction existing between cavities and the propellant matrix. A close-up look of the AP particles structure of the specimen at the strain rate of 2600 s^{-1} is shown in Fig. 5*a*. In this case, voids are initiated by AP particles debonding from the matrix. And the visible AP particles are compressed and deformed at the action of stress wave in dynamic condition.

Figure 5*b* and *c* respectively show the SEM micrographs of the specimen at the strain rate of 3300 and 4500 s^{-1}. It is evident that the compression area of single AP particle increases with the increase of the strain rate. When the strain rate increased to 4500 s^{-1}, some AP particles totally broken into pieces and fragmented, and the surface of some cavities gets worse, and finally produce cracks as shown Fig. 5*c*.

From the perspective of the microscopic observation, it is evident that the damage and crack growth mechanism

4 The macro-picture of the specimens after test under different strain rates. *a* At the strain rate of 2600 s^{-1}; *b* at the strain rate of 3300 s^{-1}; *c* at the strain rate of 4500 s^{-1}

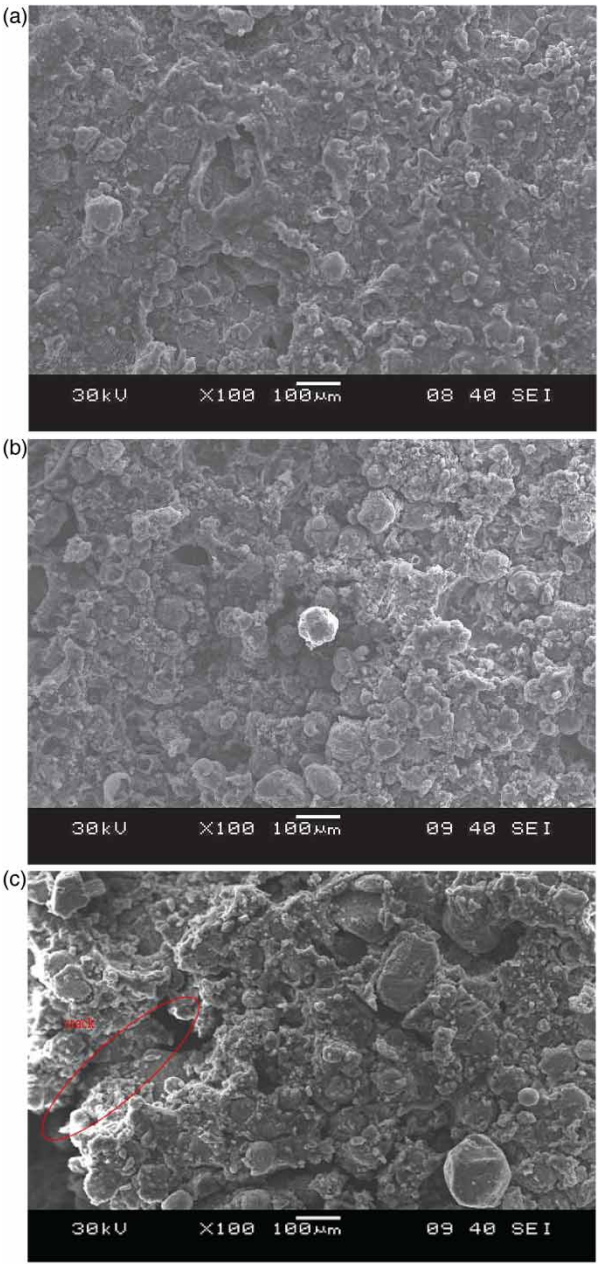

5 Typical SEM micrographs of compression surface for the specimens after test under different strain rates. *a* Represents test strain rate of 2600 s^{-1}; *b* at the strain rate of 3300 s^{-1}; *c* at the strain rate of 4500 s^{-1}

appears to include AP particles deformation. An explanation for these observed microscopy results could be the underlying mechanism of the significant rate sensitivity.

Conclusion

The dynamic compressive experiments of the aluminium–magnesium fuel-rich propellant under different strain rates have been carried out with the modified split Hopkinson pressure bar in this paper. The uniaxial compressive mechanical curves of the propellant were obtained at different strain rates of 2600, 3300, 4500 and 5100 s^{-1}. From the test curves and the electronic scanning electron microscopy images, we can get the following conclusion.

The mechanical properties of the aluminium–magnesium fuel-rich propellant are rate-dependent, and the Mg–Al fuel-rich propellant has the mechanical properties of viscoelastic material. With the increase of strain rate, the modulus of the aluminium–magnesium fuel-rich propellant obviously increases.

From a micro-structure point of view, we found the compression area of single ammonium-perchlorate particle within the propellant increases with the increase of strain rate. The specimen will produce the cracks with increasing strain rate of more than 4500 s^{-1}. The underlying mechanism of the significant rate sensitivity was explained to a certain extend by scanning electron microscopy.

Acknowledgements

This work is supported by National Pre-research Foundation of China (No.104050102). The authors would like to thank Haibin Geng, Jing Jiang and Xin Tong (Nanjing University of Science and Technology) for the help in the SHPB test.

References

1. K. Q. Wang and H. J. Mo: 'Research and development of fuel-rich propellant', *J. Aerodyn. Missile*, 2005, **35**, (11), 54–57.
2. L. L. Liu, G. Q. He and Y. H. Wang: 'Effect of oxidizer on the combustion performance of boron-based fuel-rich propellant', *J. Propul. Power*, 2014, **30**, (2), 285–289.
3. L. L. Liu, G. Q. He and Y. H. Wang: 'Thermal reaction characteristics of the boron used in the fuel-rich propellant', *J. Therm. Anal. Calorim.*, 2013, **114**, (3), 1057–1068.
4. L. L. Liu, G. Q. He, Y. H. Wang and P. J. Liu: 'Factors affecting the measurement of the percentage of gaseous products from boron-based fuel-rich propellants', *Cent. Eur. J. Energ. Mater.*, 2014, **11**, (1), 15–29.
5. Y. H. Wang, H. Cai, M. J. Wang and T. Xu: 'Analyzing the condensed-phase reaction of the combustion of fuel-rich solid propellant based on boron in low pressure', 6th International Autumn Seminar on Propellants, Explosives and Pyrotechnics, Beijing, 2005, pp. 607–610.
6. Y. H. Wang and X. H. Zhang: 'Combustion mechanism of fuel-rich propellant based on boron', 7th International Fall Seminar on Propellants, Explosives and Pyrotechnics, Xi'an, 2007, pp. 445–449.
7. Y. H. Wang, F. L. Zhang, Z. H. Sun and C. Chen, 'Improvement of combustion heat testing equipment of fuel-rich propellant based on boron', 8th International Fall Seminar on Propellants, Explosives and Pyrotechnics, Kunming, 2009, pp. 175–178.
8. Y. H. Wang, T. Xu, L. L. Liu, L. Y. Xiao and Z. X. Wang: 'Research on the combustion mechanism of boron-based fuel-rich propellant under low pressure', *Sci. Technol. Energ. Mater.*, 2014, **75**, (1–2), 21–27.
9. S. Q. Hu and B. X. Li, 'Pilot study on combustion mechanism of boron-based fuel-rich propellant', 6th International Autumn Seminar on Propellants, Explosives and Pyrotechnics, Beijing, 2005, pp. 744–746.
10. A. Kakami, R. Hiyamizu, K. Shuzenji and T. Tachibana: 'Laser-assisted combustion of solid propellant at low pressures', *J. Propul. Power*, 2008, **24**, (6), 1355–1360.
11. M. Q. Brewster and J. C. Mullen: 'Flame structure in aluminized wide-distribution AP composite propellants', *Combust. Flame*, 2010, **157**, (12), 2340–2347.
12. W. Zhang, H. Zhu, D. Y. Fang, Z. X. Xia and J. E. Xue: 'Combustion characteristics of aluminum–magnesium fuel-rich propellant', 3rd International Autumn Seminar on Propellants, Explosives and Pyrotechnics, Chengdu, 1999, pp. 262–267.
13. X. Y. Xiao, Y. L. Wang, Y. F. Liu and Z. J. Liu: 'Experimental study of combustion properties of magnesium–aluminum alloys in solid fuel-rich propellants', 7th International Fall Seminar on Propellants, Explosives and Pyrotechnics, Xi'an, 2007, pp. 592–594.
14. W. Q. Pang and X. Z. Fan: 'Study on uncertainty analyses of combustion heat for Mg/Al fuel-rich propellant', 8th International Fall

Seminar on Propellants, Explosives and Pyrotechnics, Kunming, 2009, pp. 313–316.
15. H. T. Huang, M. S. Zou, X. Y. Guo, R. J. Yang and P. Zhang: 'Analysis of the solid combustion products of a Mg-based fuel-rich propellant used for water ramjet engines', *Propellants Explos. Pyrotech.*, 2012, **37**, (4), 407–412.
16. H. Singh and R. B. Rao: 'Combustion of Mg–Zr based fuel rich propellant for air-breathing propulsion system', 1st International Autumn Seminar on Propellants, Explosives and Pyrotechnics, Beijing, 1996, pp. 215–218.
17. W. Q. Pang, X. Z. Fan and F. Q. Zhao: 'Effects of different metal fuels on the characteristics for HTPB-based fuel rich solid propellants', *Propellants Explos. Pyrotech.*, 2013, **38**, (6), 852–859.
18. L. Q. Liao, W. Q. Pang and H. X. Xu: 'Effects of different size and shaped magnesium particles on the properties for fuel rich solid propellant', *Adv. Mater. Res.*, 2013, **634–638**, 1918–1921.
19. Y. Liang, T. X. Wang and D. M. Zhang: 'Aluminum, magnesium content determination in fuel-rich propellant by potentiometric titration', 6th International Symposium on Test and Measurement, Dalian, 2005, pp. 2745–2747.
20. P. B. Wang, Z. S. Wang and Y. T. Ju: 'Experimental research on rate dependent constitutive relation of double-base propellant under impact load', *J. Solid Rocket Technol.*, 2012, **35**, (1), 69–72. (in Chinese).
21. H. Kolsky: 'An investigation of the mechanical properties of materials at very high rates of loading', *Proc. Phys. Soc. Ser. B*, 1949, **62**, (11), 676–700.
22. M. J. Forrestal, T. W. Wright and W. Chen: 'The effect of radial inertia on brittle samples during the split Hopkinson pressure bar test', *Int. J. Impact. Eng.*, 2007, **34**, (3), 405–411.
23. N. N. Dioh, P. S. Leevers and J. G. Williams: 'Thickness effects in split Hopkinson pressure bar tests', *Polymer*, 1993, **34**, 4230–4234.
24. G. T. Gray and W. R. Blumenthal: 'Split Hopkinson pressure bar of soft materials', *Mech. Test Eval.*, 2000, **8**, 488–496.
25. W. N. Chen, F. Lu, D. J. Frew and M. J. Forrestal: 'Dynamic compression testing of soft materials', *J. Appl. Mech.*, 2002, **69**, (3), 214.
26. S. Bong, Y. Ge, W. W. Chen and T. Weerasooriya: 'Radial inertia effects in Kolsky bar testing of extra-soft specimens', *Exp. Mech.*, 2007, **47**, (5), 659–670.
27. J. Zheng, Y. T. Ju, H. L. Meng and J. S. Xu, 'Numerical simulation and SHPB test study for some high polymer', 4th International Conference on Mechanical Engineering and Mechanics, Science Press: Monmouth Junction, NJ, Suzhou, 2011.